Cellulose (2023) 30:5447–5471
https://doi.org/10.1007/s10570-023-05239-z

REVIEW PAPER

Engineered transparent wood composites: a review

Thabisile Brightwell Jele · Jerome Andrew · Maya John · Bruce Sithole

Received: 11 January 2023 / Accepted: 1 May 2023 / Published online: 17 May 2023

Abstract Wood is a versatile resource due to its inherent properties such as low density, good weight to strength ratio, unique hierarchical structure, micro-scale pores, and ease of processing, including its biodegradability and renewability. In the building and construction industry, engineered transparent wood (ETW) may serve as a sustainable replacement for glass which is environmentally unfriendly in its manufacture and application. Natural wood is non transparent due to its low optical transmittance, therefore, lignin and chromophores are modified or eliminated, and a polymer is infiltrated in order to achieve transparency. Engineered transparent wood (ETW) exhibits excellent optical properties (transmittance > 80%), high haze (haze > 70%), thermal insulation (thermal conductivity less than $0.23 Wm^{-1} K^{-1}$), unique hierarchical structure, good loadbearing performance with tough failure behaviour (no shattering) and ductility. These properties extend wood applications to optical components such as solar cells, screens, windows, magnetic materials, and luminescent and decorative materials. This review details the production of ETW and how the wood density, wood thickness, wood type, wood direction, cellulose volume fraction, extent and type of delignification, polymer type, functionalisation of ETW affect the morphological, functional, optical, thermal, photodegradation and mechanical properties of ETW.

Keywords Engineered transparent wood · Delignification · Polymer

T. B. Jele (✉) · B. Sithole
Discipline of Chemical Engineering, College of Agriculture, Engineering and Sciences, University of KwaZulu-Natal (Howard Campus), Durban, South Africa
e-mail: thabisilejele94@gmail.com

T. B. Jele · J. Andrew · B. Sithole
Biorefinery Industry Development Facility (BIDF), Council for Scientific and Industrial Research (CSIR), Durban, South Africa

M. John
Centre for Nano-Structured Materials (CeNAM), Council for Scientific and Industrial Research (CSIR), Pretoria, South Africa

M. John
Department of Chemistry, Nelson Mandela University, Port Elizabeth, South Africa

Introduction

Increasing population and industrialisation worldwide cause energy shortages, high cost of energy, and environmental concerns related to the use of fossil fuels for energy generation (Li et al. 2018c). In particular, the construction sector is a major energy consumer accounting for approximately 30% of global energy usage (United Nations Environment Programme 2017; Qiu et al. 2019; Li et al. 2019b; Montanari et al. 2019). In addition, greenhouse gas emissions

emanating from the energy use of buildings are also a major concern. Consequently, there is growing interest in the construction of energy-efficient buildings that incorporate renewable, safe, and cheap building materials. The production of glass is an expensive and environmentally unfriendly process that emits 25,000 metric tons of CO_2 annually (EIA 2016; Li et al. 2019b). The high intrinsic thermal conductivity (~1 W m^{-1} K^{-1}) of glass windows in buildings causes significant heat loss (Qiu et al. 2019; Mi et al. 2020b). Glass also poses safety risks as it shatters upon impact (Li et al. 2016b; Mi et al. 2020b).

Some limitations of natural wood are due to its anisotropy, low conductivity, moisture expansion and drying, shrinkage and non-transparency caused by its low optical transmittance. Therefore, there is an urgent need to explore a more sustainable alternative to glass, such as transparent composites produced from wood, referred to as engineered transparent wood (ETW) composites. The ETW composites possess advantages such as high mechanical performance of wood along with optical properties such as transmittance and haze. Although other options such as internal and external blinds, concrete with optical fibre, transparent thermal barriers, angular selective shading systems, coatings, films, and multi-pane windows have been developed, the problem of high cost is still a major drawback (Li et al. 2018c; Mi et al. 2020b). ETW is cheap, sustainable, renewable, lightweight (low density = 1200 kg m^{-3}), and has a high fracture toughness which alleviates safety issues associated with the brittleness of glass (Li et al. 2016b, 2017a; Wang et al. 2018). Li et al. (2017a) showed that ETW had stress at break of approximately 100 MPa, which was comparable to that of glass (116 MPa). The strain at failure of ETW was 2.18% which was much higher than glass (0.19%).

The low optical transmittance of wood is due to three main factors: (1) light scattering at the interfaces between the cell wall tissue with a refractive index (RI) around 1.56 and the empty lumen pore space (RI of 1.0) in wood cells (e.g. cells such as tracheids, wood fibres, and vessels) and the presence of lignin (Li et al. 2019b; Wu et al. 2019a; Chen et al. 2020; Bisht et al. 2021); (2) light scattering due to the mismatch of refractive indices of wood components such as cellulose and hemicelluloses (both with RI of 1.53) and lignin with RI of 1.61 (Li et al. 2018a); and (3) the strong light-absorption of lignin chromophoric groups that accounts for 80–95% of the light absorption (Li et al. 2018a). In contrast, cellulose and hemicelluloses are optically colourless. In producing ETW, it is necessary to reduce light absorption by removing or modifying lignin and to minimise light scattering at the air/cell wall interface to achieve transparency (Wu et al. 2019a). Conventionally, the production of ETW entails delignification of the wood followed by infiltration of the wood ultrastructure with a refractive index-matched polymer to reduce light scattering and refractive index, suppress light reflection and increase transparency (Montanari et al. 2019). The delignified wood has a unique mesoporous cell wall structure and a high specific area (Montanari et al. 2019). The infiltrated polymer improves the mechanical strength of delignified wood by glueing wood cellulose nanofibers together (Zhu et al. 2016a). Studies have shown that ETW has excellent optical properties: transmittance > 80%, high haze > 70%, high thermal insulation (thermal conductivity less than 0.23Wm^{-1} K^{-1}) (Mi et al. 2020b), unique hierarchical structure, good loadbearing performance with tough failure behaviour (no shattering) and high ductility.(Yu et al. 2017; Yaddanapudi et al. 2017; Li et al. 2018a). In addition, ETW is lightweight, environmentally safe and mechanically stronger than unmodified wood (Wu et al. 2020). However, ETW is susceptible to weathering and photodegradation due to exposure to natural outdoor conditions such as sunlight, rain, temperature, humidity and pollutants (Bisht et al. 2021). This may cause discolouration, decrease in light transmittance, chemical degradation, microstructure breakdown and loss of mechanical properties, thereby limiting its applications (Bisht et al. 2021). For example, at a wavelength of 550 nm and UV irradiation exposure time of 0 h, 50 h, 100 h and 250 h, the light transmittance was 83%, 75%, 71% and 60%, respectively. Applications of ETW range from optical components to building materials, solar cells, and magnetic materials to luminescent and decorative materials (Fig. 1) (Gan et al. 2017a, 2017b; Yu et al. 2017; Bi et al. 2018; Li et al. 2019c; Wang et al. 2019a; Wu et al. 2020; Zhang et al. 2020; Xia et al. 2021). Montanari et al. (2019) reported successful use of ETW for thermal energy storage due to its

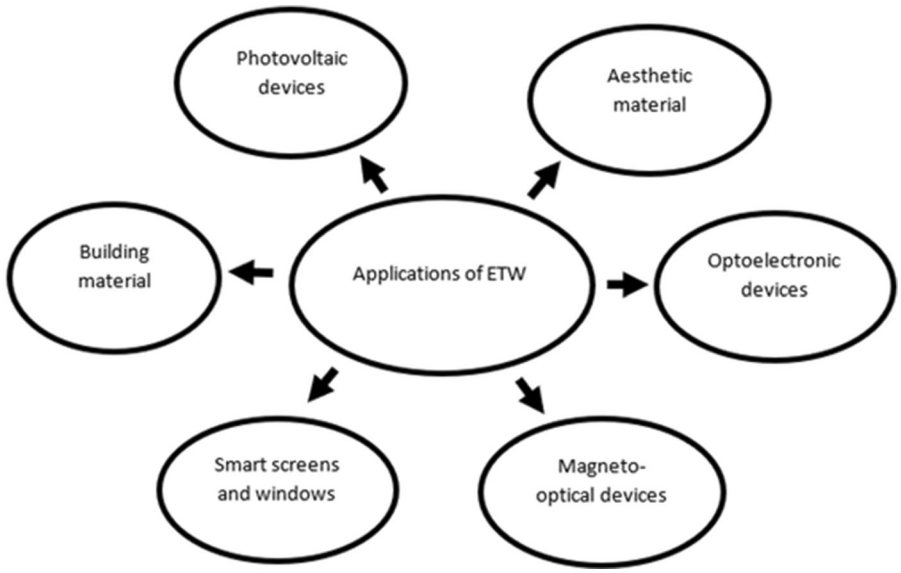

Fig. 1 Applications of engineered transparent wood composites (Li et al. 2018b, 2018c; Wan et al. 2021; Chutturi et al. 2022)

good heat storage, large latent heat of melting and crystallisation (76 J g^{-1} and 74 J g^{-1}, respectively), tunable optical transparency during phase change, and thermal insulation properties. In cases where the ETW is used as a window or roof, a consistent/uniform lighting and improved thermal insulation are guaranteed due to a combination of high optical transmittance and haze (Montanari et al. 2019). Li et al. (2019b) assembled perovskite solar cells with good long-term stability on a transparent wood substrate at low temperature (< 150℃). Even though studies have been conducted to produce ETW with excellent strength and optical properties, there is a need to improve its scalability by reducing polymer shrinkage due to polymerisation, eliminate polymer cell wall interface gaps by improving polymer infiltration, improve the short and long-term integrity of ETW, especially in outdoor applications, exploit the natural characteristics of wood to the benefit of the EWT (e.g. aesthetic patterns), and alleviate the optical constraints of ETW related to thickness by surface modification, lamination and multilayering (Jia et al. 2019; Mi et al. 2020a). Several studies detailing ETW preparation methods, optical and mechanical performance, and thermal properties references arranged in ascending order of the publication year are summarised in Table 1. This review article details the ETW production process and how the nature of wood (wood density, composition, wood directions, wood type and infiltrated polymer) affect the morphological, functional, optical, thermal, photo degradation and mechanical properties of EWT.

Production of ETW

Various techniques have been developed to produce ETW. These techniques mainly consist of two main steps: delignification or lignin modification and polymer infiltration. The schematic diagram of the production process of ETW is shown in Fig. 2. Several studies described the process of immersing a piece of wood (balsa, birch, pine etc.) in sodium chlorite in an acetate buffer solution at high temperature (80–95℃) for 6 to 12 h (Li et al. 2017a; Yaddanapudi et al. 2017; Fu et al. 2018; Qin et al. 2018). The process resulted in white coloured wood after the removal of lignin and part of the hemicelluloses because of the light scattering at the interface between the cell wall and air (Gan et al. 2017a). However, this solution-based method was long, produced a lot of liquid waste, and used large volumes of chemicals to ensure complete immersion and weakened wood. Delignified wood was characterised by delamination, fragility and instability (Li et al. 2017a). Wu et al. (2019a) performed an optimisation study of delignification time and optical properties in the production of ETW. Delignification was done using sodium chlorite in an

Table 1 A review of studies published on the production of ETW

Natural wood type and dimensions	Lignin removal	Polymer	Direction	Physical properties	Optical properties (wavelength 550 nm)	Mechanical properties and Thermal conductivity	References
Basswood	Sodium hydroxide, sodium sulfite	Epoxy		dimension = 1.4 × 3.0 × 3.5 cm	light transmittance > 85% haze ~ 95%	thermal conductivity = 0.23 Wm^{-1} K^{-1}	Li et al. (2016a)
Balsa wood 20 × 20 × 0.6 mm^3 Density of 160 kg m^{-3}	Sodium chlorite	PMMA	–	–	transmittance = 85% haze = 71%	strain- 3.9% stress ~ 90%	Li et al. (2016b)
Basswood 30 × 22 × 1 mm^3	Sodium hydroxide magnesium sulphate, hydrogen peroxide	PVP		thickness = 1 mm	light transmittance = 90% haze = 80%		Zhu et al. (2016a)
Basswood 50 × 50 × 3 mm^3	Sodium hydroxide, sodium sulfite, hydrogen peroxide	epoxy resin	longitudinal direction	thickness = 2 mm	transmittance- 80% haze- 90%	strength = 45.4 MPa modulus of elasticity = 2.4 GPa toughness = 1.2 MJm^{-3}	Zhu et al. (2016b)
			radial	thickness = 2 mm	transmittance- 80% haze- 99%	strength = 23.4. MPa modulus of elasticity = 1.22 GPa toughness = 0.59 MJm^{-3}	
Cathay poplar 20 × 20 × 0.5 mm^3	Sodium chlorite, glacial acetic acid, and hydrogen peroxide	polymethyl methacrylate, iron (III) oxide	–	–	transmittance = 63.8%	tensile strength = 40 MPa elastic modulus = 1.4 GPa strain = 5.5% stress = 42%	Gan et al. (2017a)
Basswood 20 mm × 20 mm × 0.42 mm	Sodium chlorite	PMMA	–		light transmittance = 50%	tensile strength = 152 MPa	Khalili et al. (2017)
Balsa wood 5 × 60 mm^2	Sodium chlorite	PMMA	–	–	optical transmittance = 83% and haze = 75%	stress at breakage = 100 MPa strain to failure = 2.18% % thermal conductivity = 0.23 W m^{-1} K^{-1}	Li et al. (2017a)

Table 1 (continued)

Natural wood type and dimensions	Lignin removal	Polymer	Direction	Physical properties	Optical properties (wavelength 550 nm)	Mechanical properties and Thermal conductivity	References
Beech wood thickness = 0.1 mm	Sodium chlorite	PMMA	–	–	transmittance = 70%		Yaddanapudi et al. (2017)
Balsa wood chips 20 × 20 × 1 mm^3	Diethylstilbestrol, oxalic acid and choline chloride under microwave-assisted treatment, alkaline hydrogen peroxide	acrylic acid	–	–	transmittance ~ 85% haze ~ 85%	stress ~ 27 MPa radial (R) stress ~ 60 MPa longitudinal (L)	Bi et al. (2018)
Balsa wood 2 × 2 × 0.6 cm^3	Sodium chlorite	polymethyl methacrylate	tangential		optical transmittance = 85% haze = 71%	–	Fu et al. (2018)
Birch wood	Sodium hypochlorite buffered to pH 4.6	PMMA	–	thermal conductivity = 0.23 WmK^{-1}	light transmittance ~80% haze = 70%	strain = 2.9%. stress = 140 MPa work of fracture = 3.2 MJ m^{-3}	Lang et al. (2018)
Birch wood thickness = 1.5 mm	Sodium chlorite	PMMA	–	–	non acetylated transmittance- 64% haze- 64% Acetylated: transmittance- 90% haze- 52%	–	Li et al. (2018c)
Balsa wood thickness = 1.5 mm	Sodium chlorite	PMMA	–	–	non acetylated transmittance- 83% haze- 70% acetyated: transmittance = 92% haze = 50%	–	
Balsa wood thickness = 2 mm	Sodium chlorite, hydrogen peroxide	Epoxy	–	thickness = 2 mm	transmittance = 64%	tensile strength = 75 MPa	Qin et al. (2018)

Table 1 (continued)

Natural wood type and dimensions	Lignin removal	Polymer	Direction	Physical properties	Optical properties (wavelength 550 nm)	Mechanical properties and Thermal conductivity	References
Poplar 80 × 25 × 1 mm^3	Sodium hydroxide magnesium sulphate, hydrogen peroxide	PMMA	–	–	transmittance = 92% haze = 56%		Wang et al. (2018)
Balsa wood 20 × 20 × 5.9 mm^3 density = 120 kg m^{-3}	Sodium chlorite acetate buffer solution, acetic anhydride	PMMA	–	–	non-acetylated transmittance ~ 40% acetylated transmittance ~ 52%		Chen et al. (2019)
Basswood 100 × 100 × 1.6 mm^3 density = 401 kg m^{-3}	Sodium chlorite	photocurable methacrylate resin	longitudinally	thickness = 3.41 mm—2ply acetylated	acetylated: transmittance = 46%, haze 89% elastic modulus = 7 GPa tensile strength = 40 MPa Non acetylated: transmittance = 38%, haze 90%, elastic modulus = 6.5 GPa, Tensile strength = 75 MPa	acetylated: elastic modulus = 7 GPa, Tensile strength = 40 MPa non-Acetylated: elastic modulus = 6.5 GPa tensile strength = 75 MPa	Foster et al. (2019)
Basswood blocks with a density of 455 kg m^{-3} thickness = 0.71 mm	Sodium hypochlorite	epoxy resin	longitudinal direction	density = 109 000 kg m^{-3}	transmittance = 91.5% haze = 10.1%	tensile strength = 43.4 MPa elongation at break = 19.14% toughness = 6.10 MJ m^{-3}	Jia et al. (2019)
Basswood 50 × 50 × 5 mm	Hydrogen peroxide	epoxy resin	–	Thickness = 0.5 cm	light transmittance ~ 87% haze ~ 90%	strength ~ 20 MPa stress ~ 20 MPa strain ~ 3.2	Li et al. (2019a)
–	Sodium chlorite	PMMA	–	thickness = 1 mm	light transmittance = 86% Haze ~ 70%	thermal conductivity = 0.23 W m^{-1} K^{-1}	Li et al. (2019b)

Table 1 (continued)

Natural wood type and dimensions	Lignin removal	Polymer	Direction	Physical properties	Optical properties (wavelength 550 nm)	Mechanical properties and Thermal conductivity	References
Balsa wood $250\times250\times15$ mm^3	Sodium hydroxide, sodium sulfite	PMMA	–	–	transmittance = 75% haze = 85%	fracture strength = 31.9 MPa modulus = 5.26 GPa	Li et al. (2019c)
Silver birch wood $20\times20\times0.5$ mm^3 density 620 kg m^{-3}	Sodium chlorite	PMMA	–	thickness = 0.5 mm	transmittance = 80% haze = 80%	strength = 71 MPa elastic modulus = 14.9 GPa thermal conductivity = 0.30 Wm^{-1} K^{-1}	Montanari et al. (2019)
Poplar wood $25\times25\times1$ mm^3	Sodium chlorite	PMMA	–	–	transmittance = 40%	high fracture strength = 96.4 MPa modulus = 4.27 GPa thermal conductivity = 0.2 Wm^{-1} K^{-1}	Qiu et al. (2019)
Poplar wood (Populus deltoides) $20\times20\times1$ mm^3	Sodium hydroxide magnesium sulphate, hydrogen peroxide	PVA			transmittance = 80% haze = 90%	fracture strength = 13.3 MPa elastic modulus = 0.26 GPa	Rao et al. (2019)
Balsa wood slice 40×20 mm^2	Sodium hydroxide and sodium sulfite solution	polymerizable deep eutectic solvents, acrylic-acid, choline chloride	longitudinal	thickness = 0.35 mm	transmittance = 80%	young modulus = 2.08 MPa	Wang et al. (2019b)
Basswood	Sodium chlorite	–	–	thickness = 0.42 mm	optical transmittance = 61%		Wu et al. (2019b)
Basswood	Hydrogen peroxide, trisodium citrate dihydrate, sodium hydroxide	PMMA	–	–	transmittance = 30%	tensile strength = 165 MPa	Wu et al. (2019c)

Table 1 (continued)

Natural wood type and dimensions	Lignin removal	Polymer	Direction	Physical properties	Optical properties (wavelength 550 nm)	Mechanical properties and Thermal conductivity	References
Balsa wood density of 90—110,000 kg m^{-3} 15 × 15 × 0.9—1.2 mm^3 Cellulose volume fraction = 4.3	Sodium silicate, sodium hydroxide, magnesium sulfate, diethylenetriaminepentaacetic acid and hydrogen peroxide	trifunctional ene monomer, tetrafunctional thiol monomer, UV-initiator 1-hydroxy-cyclohexyl phenyl ketone	–	–	transmittance = 90% haze = 36%	tensile strength = 59.0 MPa modulus = 3.4 GPa stress- 60 MPa strain- 2.5%	Höglund et al. (2020)
Balsa wood with a density of 90 000 − 110 000 kg m^{-3} 15 × 15 × 0.9 − 1.2 mm cellulose volume fraction = 5.0 ± 0.1	Sodium chlorite	trifunctional ene monomer, tetrafunctional thiol monomer, UV-initiator 1-hydroxy-cyclohexyl phenyl ketone	–	–	transmittance = 85% haze = 63 ± 0.7%	tensile strength = 53.7 MPa modulus = 3.2 GPa stress- 55 MPa strain- 2.5%	
Birch density = 1500 kg m^{-3}	Sodium chlorite	poly(methyl methacrylate) (PMMA)	–	thickness = 1.3 mm	optical transmittance = 70%	modulus = 9 GPa and ultimate strength of 263 MPa	Jungstedt et al. (2020)
douglas fir 60 × 60 × 2 mm^3	Sodium chlorite	Epoxy	–	–	transparency ~ 80% haze ~ 93%,	strength of 92 MPa, high toughness of 2.73 MJm^{-3} thermal conductivity = 0.24 Wm^{-1} K^{-1}	Mi et al. (2020a)
Balsa wood	Sodium hypochlorite	PVA	–	–	transmittance = 91% haze = 15%	toughness = 3.03 MJ m^{-3} Thermal conductivity = 0.19 W m^{-1} K^{-1}	Mi et al. (2020b)
Poplar wood veneers 100 × 30 × 2 mm^3	Sodium hydroxide, magnesium sulfate, hydrogen peroxide, Ethylenediaminetetraacetic acid, disodium salt	epoxy resin doped with a UV absorber	–	–	transmittance = 83.53% haze ~ 95%		Bisht et al. (2021)

Table 1 (continued)

Natural wood type and dimensions	Lignin removal	Polymer	Direction	Physical properties	Optical properties (wavelength 550 nm)	Mechanical properties and Thermal conductivity	References
Balsa wood $50\times50\times1.01$ mm^3	Sodium hydroxide and sodium sulfite solution	epoxy	–	dimensions = $50\times50\times1.2$ mm^3	transmittance = 80% transmittance = 65% with indium tin oxide	–	Cho et al. (2021)
Balsa wood 304 kg m^{-3}	Aqueous PAA solution	limonene acrylate monomer		at 1.2 mm thickness	transmittance = 90% Haze = 30%,	strength = 174 MPa, Young's modulus 17 GPa	Montanari et al. (2021)
New Zealand pine = 330 kg m^{-3}, thickness = 0.5 mm	Sodium hypochlorite solution	PMMA	3 ply -same direction	–	transmittance ~ 9%	tensile strength = 50 MPa	Wu et al. (2021)
basswood 0.42 kg m^{-3}, thickness = 0.5 mm	Sodium hypochlorite solution	PMMA	3 ply -same direction	–	transmittance ~ 6%	tensile strength-50 MPa	
Balsa wood $200\times10\times0.6$ mm^3	Hydrogen peroxide brushing solar illumination	epoxy	thickness = 1 mm	–	light transmittance ~ 90% high haze ~ 60%	tensile strength (46 MPa for L and 31 MPa for T), toughness of L 0.93 and T 1.64 MJ m^{-3}	Xia et al. (2021)

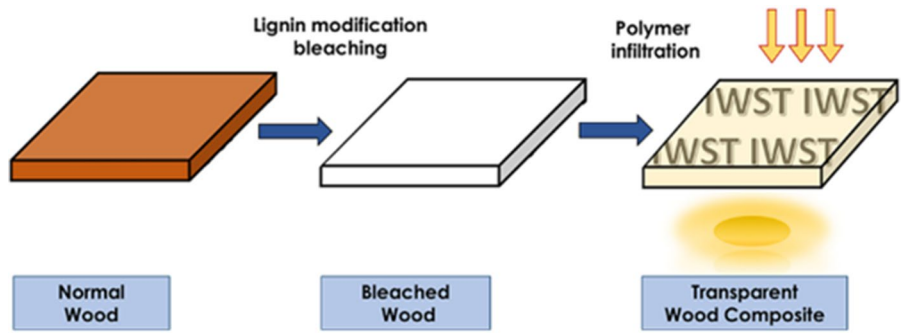

Fig. 2 Production process of ETW. Reproduced with permission Copyright 2018, John Wiley and Sons (Bisht et al. 2021)

acetate buffer solution, and the delignification time was varied from 30 to 150 min at 30 min intervals. The maximum optical transmittance achieved was 61% at 800 nm for ETW with 9% lignin content at 150 min delignification time and with methyl methacrylate (MMA) impregnation and polymerisation. The drawbacks of using sodium chlorite were the production of toxic gases and yellowing when lignin reached equilibrium point (Qin et al. 2018). Qin et al. (2018) obtained transparent ETW with 82% light transmittance from 2 mm thick balsa wood delignified by a two-step partial delignification process using 1 wt% sodium chlorite followed by treatment with 5 mol L^{-1} hydrogen peroxide to prevent yellowing. Li et al. (2017a) modified lignin by only removing the chromophores using hydrogen peroxide from balsa wood. The process was less toxic because hydrogen peroxide is an oxidant that produces only water as a by-product, notably reducing waste liquid production. Eliminating chromophores resulted in highly stable, rigid, well-preserved bleached wood with 80% lignin retention (Li et al. 2017a; Bisht et al. 2021). However, on the downside, high amounts of chemical, water, and energy consumption were noted. Partial delignification was reported to endow the ETW with color and texture for decoration, where absolute transparency was not a priority (Wu et al. 2020). In order to minimise chemical consumption during delignification, Xia et al. (2021) performed a brushing technique on 0.6 mm balsa wood with hydrogen peroxide which preserved the aromatic backbone of lignin but diminished its chromophore content. This was followed by a clear epoxy infiltration into pores using vacuum. ETW with a transmittance > 90%, high haze > 60%, excellent light-guiding over visible wavelength, patternable surface, excellent tensile strength (46.2 MPa for L and 31.4 MPa for T), toughness of L (0.93 MJ m^{-3}) and T (1.64 MJ m^{-3}) was produced (Xia et al. 2021). Bi et al. (2018) used a low-cost green eutectic solvent to break the bonds between lignin and carbohydrate in 1 mm thick balsa wood under a microwave assistant treatment. The ETW produced by acrylic acid infiltration had light transmittance and haze of 85% and 85%, respectively. Li et al. (2019a) delignified basswood with 30 wt% hydrogen peroxide steam, which penetrated the wood cells and removed lignin together with other dissolved degradation products. The epoxy resin infiltrated ETW of 0.5 mm thickness and had a light transmittance and haze of 87% and 90% respectively.

Various types of polymers used in the production of ETW include epoxy resin polyethylene oxide (PEO), polyvinylpyrrolidone (PVP), polydimethylsiloxane (PDMS), styrene, vinyl carbazole, isobornyl methacrylate and poly(methyl methacrylate) (PMMA) (Bi et al. 2018). Although PMMA has high optical transparency, its main drawback is the lack of compatibility between the polymer and the cell wall of the delignified wood and a refractive index (RI) mismatch with wood (RI is 1.49 for PMMA and 1.53 for holocellulose) leading to decreased transparency and mechanical properties (Li et al. 2018c). Qiu et al. (2019) used a combination of PMMA and antimony tin trioxide (ATO), resulting in improved mechanical properties, although the transparency of polar wood was reduced (Qiu et al. 2019). ATO was composed of hydrophilic groups in the silane coupling, which improved interfacial bonding between PMMA and the delignified wood. Li et al. (2018c) achieved 1.5 mm thick ETW with an optical transmittance of 92% (in the visible wavelength range) by surface application of acetylation on delignified wood substrates followed by PMMA infiltrations. Acetylation reduced the hydrophilicity of wood, thus improving

compatibility between the wood template and PMMA and promoting interface bonding. For 3 mm thick acetylated and non-acetylated ETW, the optical transmittance obtained was 89% and 60%, respectively. In addition to improved optical properties, acetylated ETW exhibited a higher work of fracture (1.0 MJ m^{-3}) compared to glass and a higher modulus of 4 GPa and stress at break of 78.9 MPa compared to the original wood and PMMA. It was concluded that the improved mechanical properties were attributed to the strong interaction between wood and PMMA facilitated by acetyl groups (Li et al. 2018c).

Wood density

The density of wood can vary significantly depending on the type of species. For instance, Balsa is the lowest density tree species (120 kg m^{-3} to 160 kg m^{-3}), largely due to its fast growth (Qin et al. 2018; Li et al. 2019b). Populus deltoids is a porous and thin cell walled wood with large cell cavities and short fibres hence its relatively low density of 460 kg m^{-3} (Chen et al. 2019). After delignification, the density further decreased to 400 kg m^{-3} due to the enhancement of the wood cell wall porosity after the removal of lignin, hemicellulose and amorphous cellulose. After polymer infiltration into the pores, the ETW increased to 1198 kg m^{-3}. Wang et al. (2021) confirmed the density of ETW (1221 kg m^{-3}) to be higher than that of delignified wood (67 kg m^{-3}) and natural balsa wood (121 kg m^{-3}). Balsa wood of density 126 kg m^{-3} was delignified by sodium chlorite at pH 4.6 and reduced to a density of 65 kg m^{-3}. After polymer impregnation the density increased to 1232 kg m^{-3} (Wang et al. 2022). Low-density wood such as pine, ash, and poplar are suspectable to breakage after lignin removal (Li et al. 2017a). Lignin acts as a binder between wood cells, hence the loss in the mechanical integrity of wood after delignification (Mi et al. 2020a). Qin et al. (2018) compared the properties of low-density balsa wood (210 kg m^{-3}) (Ochroma pyramidale) and higher density of basswood (490 kg m^{-3} Tilia tuan). The tensile strength of transparent high density basswood (8.1 MPa) was higher compared to low density balsa wood (6.1 MPa) with a thickness of 2 mm. Wu et al. (2020) conducted a comparative study of the optical properties of ETW produced from two different wood species (*Betula alnoides* (Betula) and New Zealand pine (*Pinus radiata* D. Don) of different densities and equal thickness. The light transmittance of *Betula alnoides* with a density of 680 kg m^{-3} and New Zealand pine with a density of 310 kg m^{-3} was increased by 11.34% and 14.4%, respectively. Qin et al. (2018) confirmed that the transmittance of the ETW decreased as the original wood density increased. For instance, the light transmittance of balsa with a density of 210 kg m^{-3} and balsa with a density of 490 kg m^{-3} was 77% and 64%, respectively. Mi et al. (2020a) demonstrated successful production of tunable aesthetic wood with UV blocking properties from Douglas fir softwood exhibiting annual growth ring patterns of macroscopic and microscopic scales. The two variations in patterns of Douglas fir were termed low density (284 kg m^{-3}) early wood (EW) and high density (846 kg m^{-3}) latewood (LW). However, the preservation of the natural wood aesthetic in hardwood (e.g., basswood, balsa) was not possible owing to its uniform bimodal pores, large lumen diameter and uniform and thinner cell walls (approx. 1.3–2.9 µm) compared to softwood (approx. 5–10 µm for LW). Also, ETW of softwoods, with a cell wall thickness of 1.4–2.6 µm, was not as successful in preserving the natural aesthetic of natural wood upon delignification as LW owing to the faster solution diffusion in EW. Furthermore, a comparative study of wood cut by different methods (cross section and quarter slicing cutting strategies) to achieve two directions [microchannels perpendicular (R-wood) or parallel to the wood plane (L-wood)] was conducted. Delignification was done for 2 h using sodium chlorite in acidic conditions in order to preserve lignin which endowed ETW with UV blocking properties through its phenylpropane structures and phenolic hydroxyl groups. Epoxy was used as a polymer to produce ETW. The mechanical properties of ETW from L wood (tensile strength of 92.0 MPa, toughness of 2.73 MJ m^{-3}) were much higher than for both R wood (tensile strength of 21.60 MPa, toughness of 0.523 MJ m^{-3}) and natural wood (tensile strength of 6.24 MPa). It was concluded that the high mechanical properties of L-ETW were due to the improved synergy between the wood template and the polymer (Mi et al. 2020a). Li et al. (2018c) reported that acetylated ETW produced from wood of high density, had improved transmittance compared to lower density wood. Rao et al. (2019) reported that the density of native poplar veneer only increased from 380 kg m^{-3} to 910 kg m^{-3} after polymer impregnation due to

shrinkage of polyvinyl alcohol (PVA) and deformation of the lignin modified wood template during PVA drying. Mi et al. (2020a) reported that delignification of high-density hardwood takes a longer time than low density softwood.

Cellulose volume fraction

The cellulose volume fraction of wood was calculated according to Eqs. 1 and 2 (Li et al. 2016b).

$$V_f = \frac{W_{f\times\rho_c}}{\rho_f} \tag{1}$$

$$\rho_c = 1/\left(\frac{W_f}{\rho_f} + \frac{W_m}{\rho_m}\right) \tag{2}$$

where V_f is the volume fraction of cellulose, ρ_c is the density of ETW, ρ_f is the density of holocellulose (1500 kg m^{-3}), ρ_m is the density of the polymer, W_m is the weight fraction of the polymer, and W_f is the weight fraction of cellulose.

The cellulose volume fraction in wood is a tunable property that has an effect on the properties of ETW. Fu et al. (2018) reported a linear relationship between the strength of ETW with cellulose volume fraction. For instance, the ultimate strength of ETW with a cellulose volume fraction of 5%, 12.5% and 20% was approximately 40 MPa, 62 MPa and 90 MPa, respectively. Jia et al. (2019) studied the effect of thickness and cellulose volume fraction on the optical properties of ETW. They found that the transmittance of ETW with cellulose volume fractions of 2.89%, 5.86% and 8.71% was approx. 90%, whereas the haze gradually increased to 5%, 10% and 41.6%, respectively. Li et al. (2018c) reported that non-acetylated ETW of a thickness of 1.5 mm, made from birch wood with 30% cellulose by volume, had a transmittance of 64%, while acetylated ETW had a transmittance of 90%. A lower volume fraction of wood of 5% had a transmittance of 83% and 92% for non-acetylated and acetylated ETW, respectively. It was concluded that a high-volume fraction of cellulose resulted in light-scattering originating from the cellulosic cell wall (Li et al. 2016b). An increase in cellulose volume fraction from 5 to 65% resulted in a decrease in transmittance from 85 to 34.6% (Li et al. 2019b). The cellulose volume fraction and cell wall porosity were increased by compression of delignified wood. For instance, Li et al. (2016b) increased the cellulose volume from 5 to 19% by compression of delignified balsa wood. Compression is also important in tailoring wood to the desired thickness.

Wood thickness

Wood thickness and its direction has a direct effect on optical transmittance and haze (Li et al. 2018c). The thinner the wood sample, the higher its light transmittance and the lower its haze (Li et al. 2018a; Qin et al. 2018; Kanócz et al. 2020). Zou et al. (2022) confirmed that an increase in thickness resulted in an increase in haze due to longer light pathways and increased scattering centres. Figure 3 illustrates the decrease in transparency of ETW with an increase in thickness.

Kanócz et al. (2020) reported a dependence of light transmittance on both the thickness and volume fraction of cellulose. Chen et al. (2019) studied the dependence of the optical transmittance of acetylated and non-acetylated ETW on thickness using the anisotropic photon diffusion equation and an equation that quantifies the total transmittance (see Eq. 3). An exponential relationship between

Fig. 3 Photographs of ETW of varying thickness. Reproduced with permission Copyright 2018, John Wiley and Sons (Vasileva et al. 2018)

the total transmittance and sample thickness was observed (Chen et al. 2019).

$$T_{total} = \exp\left(-\sqrt{\left(\frac{D_{xy}}{D_x}\right)^{\frac{1}{6}} \frac{\mu c}{D_{xy}}} d\right) \quad (3)$$

where T_{total} is total transmittance, μ is the isotropic absorption, c is the speed of light in ETW samples, D_{xy} is the diffusion coefficients perpendicular to the wood fibres, and d is the sample thickness.

Lower thickness resulted in higher optical transmittance because a shorter light pathway lowers light attenuation and vice versa (Montanari et al. 2019). For instance, 1 mm thick ETW had a transmittance of 85% in the radial direction, 2 mm thick ETW had a transmittance of 80% with thickness perpendicular to the longitudinal direction, and 3 mm thick ETW had a transmittance of 90% with thickness in the longitudinal direction (Zhu et al. 2016b; Li et al. 2018c). The transmittance of 0.7 mm and 1.5 mm thick ETW was approx. 90%, whereas haze was 10% and 30%, respectively (Li et al. 2016b). The transmittance of acetylated ETW of thickness 1.5 mm, 3 mm, 7 mm and 10 mm was 92%, 89%, 70% and 60% at a wavelength of 550 nm, respectively (Li et al. 2018c). The optical haze of acetylated ETW of thickness 1.5 mm, 3 mm, 7 mm and 10 mm was approximately 80%, 75%, 50% and 45%, respectively. Chen et al. (2019) compared the differences in transmittance for acetylated and non-acetylated ETW. They found that the transmittance of acetylated ETW of thickness 0.24 cm, 0.32 cm, 0.42 cm, 0.51 cm, and 0.65 cm was 86%, 82%, 77%, 72% and 66% at a wavelength of 550 nm, respectively. Non-acetylated ETW had transmittance values of 84%, 72%, 65%, 62%, 51% and 44% for samples of thickness 0.11 cm, 0.21 cm, 0.25 cm, 0.31 cm, 0.43 cm and 0.46 cm respectively. The light transmittance of 1.5 mm and 2 mm ETW was 80% and 77%, respectively (Qin et al. 2018). ETW is highly anisotropic due to its oriented fibrous structure. Correspondingly, an ETW sample will scatter light differently along two directions (transverse and longitudinal) depending on the light propagation direction (Vasileva et al. 2018). Li et al. (2016b) reported a light transmittance of 90% and 40% for ETW of thickness 0.7 mm and 3.7 mm respectively.

In contrast, optical haze increases with an increase in thickness. Acetylated ETW of thickness 1.5 mm and 3 mm had an optical haze of 50% and 53%, respectively. Non -acetylated ETW of thickness 1.5 mm and 3 mm had an optical haze of 70% and 78%, respectively. The lower optical haze for acetylated ETW was attributed to the improved compatibility between wood and PMMA, resulting in lower light scattering. Rao et al. (2019) reported a decrease in breath and thickness of ETW due to the simultaneous convergence of contracted wood cells. The length, breadth and thickness of the original wood and ETW were $20\times20\times1$ mm^3 and $20\times16\times0.7$ mm^3, respectively. However, the addition of propylene glycol (PG) maintained the lumen and shape of ETW by reducing internal wood stresses, resulting in a sample with dimensions similar to those of original wood, i.e. $20\times17\times0.9$ mm^3 for 50 wt% PG-ETW and $20\times18\times0.9$ mm^3 for 100 wt% PG-RTW (Rao et al. (2019). Wood thickness also affected the duration of delignification. Basswood cut in a direction perpendicular to the wood plane of thickness 20 nm and 40 nm was delignified with hydrogen peroxide and hydrogen acetate steam to a white colour after 4 and 20 h, respectively (Li et al. 2019a).

Type of wood

Wood species have varying densities, cellulose contents, cell structural morphologies, and annual ring structures, all of which affect the structural, mechanical, functional and optical properties of ETW (Rao et al. 2019). Examples of wood species that have been used to produce ETW are balsa, basswood, cathay poplar, pine, birch, and ash (Li et al. 2016b, 2017b, 2017a; Zhu et al. 2016a; Gan et al. 2017b). Figure 4 shows ETW produced from balsa, pine, birch, and ash by the lignin modification process and PMMA infiltration (Li et al. 2017a). Li et al. (2019a) conducted a comparative study on the effect of delignification on two wood species (i.e., basswood and pine) cut in the direction aligned either perpendicular to (Ra) or along (Ro) the wood plane. Basswood had a unique multichannel structure with ultra-thin channel walls and low density. As a result, a longer time (8 h lignin modification and 18 h $NaClO_2$ process) was needed to achieve delignification, compared

Fig. 4 Images of ETW produced from balsa, pine, birch, and ash. Reproduced with permission Copyright 2017, John Wiley and Sons (Li et al. 2017a)

to pine which required 4 h. Wu et al. (2021) fabricated multi-layered ETW from two different wood types, i.e., New Zealand pine and Basswood, of densities 330 kg m^{-3} and 420 kg m^{-3}, respectively and thickness of 0.5 mm. The three-layered ETW were arranged either in the same direction or alternating directions (the first layer and the third layer were in the same direction) according to fibre directions for each type of wood studied. Each type of wood studied was partially delignified using $NaClO_2$ followed by PMMA infiltration into the three layered delignified wood samples. The light transmittance (wavelength = 550 nm) for the three-layered New Zealand pine and basswood ETW arranged in the same direction according to wood fibres was 8% and 6%, respectively. On the other hand, the light transmittance of the three-layered New Zealand pine and basswood ETW arranged in alternating directions was 4% and 3%, respectively. The tensile strength of the three layered ETWs in the same direction and in different directions was approximately 50 MPa and 40 MPa, respectively, for each of the wood species studied. Original New Zealand pine and Basswood had tensile strengths of approx. 37 MPa and 39 MPa for the same direction and approx. 30 MPa and 32 MPa for different directions, respectively. In another study, Foster et al. (2019) compared the optical and mechanical properties of acetylated and non-acetylated single ply and double-ply ETW in an effort to improve mechanical properties and alleviate thickness constraints on ETW. Basswood of thickness 1.6 mm and density 410 kg m^3 was delignified, acetylated and infiltrated with PMMA. Two-ply ETW was arranged with one ply in the same direction as the fibre alignment and the other ply positioned 90° transverse to the fibre alignment. The optical properties of acetylated ETW (transmittance = 46%, haze 89%) were superior to those of non-acetylated ETW (transmittance = 38%, haze = 90%). On the other hand, the elastic modulus of acetylated ETW (7 GPa) was slightly greater than non-acetylated, whereas the tensile strength of non-acetylated ETW (75 MPa) was much greater than acetylated ETW (40 MPa). However, for single-ply ETW, the mechanical properties of acetylated ETW (elastic modulus = 4 GPa, tensile strength = 15 MPa) were much higher than for non-acetylated ETW elastic modulus = 3.5 GPa, tensile strength = 10 MPa) positioned 90°/transverse to fibre alignment.

Wood direction

The optical properties of wood are direction dependant due to its anisotropic nature. The way in which wood is sawn affects its cellulose volume fraction, which in turn affects the optical transmittance of ETW. Radially sawn wood and longitudinally sawn wood have a low and high-volume fraction of cellulose, respectively (Kanócz et al. 2020). Low and high volume fraction wood with a thickness of 2 mm exhibits an optical transmittance of 90% and 80%, respectively (Li et al. 2016b). Zhu et al. (2016b) compared the mechanical properties of transparent radially and longitudinally sawn wood to that of their natural counterparts. The fracture strength of transparent longitudinally cut wood strength (45 MPa) was almost twice that of transparent radially cut wood (23 MPa). The fracture strength of natural radially and natural longitudinally cut wood was 4.5 MPa and 42 MPa, respectively (Zhu et al. 2016b). These results were similar to those obtained by Wang et al. (2021), where the mechanical properties of longitudinal ETW (fracture strength = 23 MPa, elastic modulus = 666 MPa, and toughness = 728 kJ m^{-3}) were greater than transverse ETW (fracture strength = 2.6 MPa, elastic modulus = 46 MPa, and toughness = 320 kJ m^{-3}). The scanning electron microscope (SEM) analysis revealed that in longitudinal ETW, a 3D network was formed due to the interaction of cellulose nanofibers in delignified wood (DW) and the polymer, hence the high mechanical strength compared

to transverse ETW which exhibited weak bonding interfaces between the wood tissue and the polymer. However, R-ETW had an higher optical transmittance of 73.3% than L-ETW with 68.2% (Zhu et al. 2016b; Zhang et al. 2020). It was concluded that the polymer had better compatibility with R-wood due to the small depth of the lumina (Zhu et al. 2016b). Wang et al. (2022) reported thermal conductivities of 0.3 mW m^{-1} K^{-1} and 0.29 mW m^{-1} for transverse and longitudinal editable shape-memory ETW, respectively. Zhang et al. (2020) confirmed the difference in thermal conductivities by producing radial ETW and longitudinal ETW with thermal conductivities of 0.32 W m^{-1} K^{-1} and 0.20 W m^{-1} K^{-1}, respectively. The difference in thermal conductivity values is due to well preserved wood cells even after the delignification process resulting in anisotropic thermal properties. (Li et al. 2016a). Mi et al. (2020a) reported anisotropic thermal properties for axial-ETW and radial-ETW. Radial-ETW and axial ETW had thermal conductivities of 0.24 W m^{-1} K^{-1} and 0.41 W m^{-1} K^{-1}. It was concluded that restrained heat transfer in the radial direction results in greater light scattering than in the axial direction. Further comparison was made between epoxy polymer, ETW and glass. The thermal conductivity of epoxy (0.29 W m^{-1} K^{-1}) was slightly less than that of ETW (0.3 W m^{-1} K^{-1}) and glass (0.86 W m^{-1} K^{-1}). The low thermal conductivity of ETW was due to the low transmission of photon in the wood fibre (Li et al. 2016a). The study of the effect of temperature on the thermal conductivities of transverse ETW showed an increase in thermal conductivity from 0.29 W m^{-1} K^{-1}, 0.3 W m^{-1} K^{-1} to 0.32 W m^{-1} K^{-1} at 0 °C, 25 °C and 50 °C, respectively. However, the conductivities remained far less than that of glass. It was concluded that ETW is a more efficient thermal insulator than glass, therefore, making it a suitable alternative in energy efficient buildings (Wang et al. 2022). The same trend was reported by Zou et al. (2022), where the pectin-PMMA ETW had a thermal conductivity of approximately 0.1 Wm^{-1} K^{-1} far less than that of glass (~0.9 Wm^{-1} K^{-1}). However, the thermal conductivity of PMMA (approx. 0.2 Wm^{-1} K^{-1}) was slightly higher than that of pectin-PMMA-ETW (Zou et al. 2022). Longitudinal ETW is characterised by the propagation of light perpendicular to the wood longitudinal direction, high interface density (number of interfaces per length), high transmittance, low haze, isoptropic light scattering effect and low density of polymer/cellulose interfaces due to the hollow cylinder shape of wood cells. In contrast, transverse wood is characterised by propagation of light in the transverse plane and with low interface density. Longitudinal wood exhibits isotropic light scattering whereas transverse wood exhibits anisotropic light scattering at the wood cell wall and polymer interface. Moreover, light scattering of longitudinal wood has a balanced angular distribution in both the x and y direction, whereas a larger scattering angle in the y direction compared to the x direction was observed for transverse wood (Li et al. 2018a).

Degree and type of delignification process

A fast, environmentally friendly, lignin preserving and mechanical strength preserving delignification/modification method is the most favourable in the production of ETW (Li et al. 2017a). In addition, the delignified wood should be strong enough to allow easy handling during polymer infiltration (Li et al. 2018a). The delignification of wood creates nano and microscale voids in the cell wall, which leads to increased specific surface area from 1.2 m^2 g^{-1} to 20 m^2 g^{-1} in natural wood (Li et al. 2018a). Li et al. (2019a) reported the complete removal of lignin using hot hydrogen peroxide and hydrogen acetate solution to a concentration as low as 0.84%, resulting in increased pores in the cell wall corners, which allowed for more efficient epoxy resin infiltration, high cellulose retention, suppressed interface debonding gaps, high transmittance (87%), high haze (90%), and mechanical strength of ETW. Delignification mainly affects the colour of the natural wood. The methods of delignification include bleaching by total immersion with 1 wt% of sodium chlorite in acetate buffer solution (pH 4.6) at 80 °C (Li et al. 2018c), two step delignification with 1 wt% of sodium chlorite in acetate buffer solution (pH 4.6) at 80 °C sodium chlorite followed by 5 mol L^{-1} hydrogen peroxide at 90 °C (Qin et al. 2018), 30 wt% H_2O_2 brushing followed by solar illumination (Xia et al. 2021), lignin chromophore removal using alkaline H_2O_2 hydrothermal solution (Li et al. 2017a), 2 step delignification with NaOH and sodium sulphate followed by hydrogen peroxide and hydrogen peroxide and hydrogen acetate steaming (Wang et al. 2019a). The measures of delignification are lignin content, lightness, redness and yellowness

(Wu et al. 2019a). Chemical delignification methods are time consuming and operated at high temperatures. For instance, Yaddanapudi et al. (2017) delignified beech wood with thickness 0.1 mm using 5 wt % sodium chlorite in an acetate buffer solution at 95 °C for 12 h. Qin et al. (2018) opted for a 2 step partial delignification and an optimum time of 3 h $NaClO_2$ and 1 h H_2O_2 treatment for 1 mm thick balsa wood. However, the delignification time required increased with increase in wood thickness. $NaClO_2$ treatment times of 4 h, 5 h and 12 h were recorded for balsa woods of thickness 1.5 mm, 2 mm, and 5 mm, respectively. Xia et al. (2021) avoided using large amounts of chemicals and producing liquid waste streams by using H_2O_2 brushing instead of delignification by immersion. The ETW produced had a transmittance > 90%, high haze > 60%, and an excellent light guiding over the visible wavelength. Furthermore, the strength of the ETW was 50 times more superior than ETW obtained by delignification by immersion. Wu et al. (2019a) studied the effect of the extent of delignification of basswood on the morphological, optical and mechanical properties of transparent wood production. The lightness of transparent wood increased with delignification, while the redness and yellowness decreased (Wu et al. 2019a). The surface colour was the most obvious observation of ETW samples of different lignin contents (viz., 16%, 15%, 13%, 12% and 9%). Unmodified wood (with 24% lignin content) had a yellowness value of 52.5, while the yellowness values of the ETW samples decreased to approximately 25, 21, 19, 18, and 15, respectively. In contrast, the lightness increased from 69.5 for unmodified wood to 80, 85, 87, 88, and 90 for the ETW samples, respectively. The optical transmittance of the ETW samples increased with an increase in the degree of delignification (Qin et al. 2018; Wu et al. 2019a). For instance, unmodified wood and the most delignified wood (lignin content of 9%) had optical transmittance values of 0% and 61% at a wavelength of 800 nm, respectively. Mechanical properties of the ETW were negatively affected by increased levels of delignification. The tensile strength decreased with a decrease in lignin content in ETW samples. The highest tensile strength was reported for the ETW sample with a low degree of delignification (15% lignin content). Additionally, delignified wood was reported to have lower tensile strength value compared to their respective ETW samples, indicating that polymer impregnation of MMA contributed to the final improvement of mechanical strength of ETW samples. It was concluded that the pores created by the removal of lignin were responsible for the improvement of light transmittance in samples (Wu et al. 2020). Li et al. (2017a) compared the wet strength measured perpendicular to the fibre direction of various wood species (balsa, birch, pine and ash) with thickness 1.5 mm as a measure of the stability that were delignified by either lignin removal or lignin modification. The wet strength of balsa with a lignin content of 21.3% (lignin modified) and 2.5% (lignin removed) was 7.9 MPa and 6.9 MPa, respectively. Lignin modified (lignin = 20.1%) and delignified Birch wood (lignin = 3.3%) had a wet strength of 14.4 MPa and 1.4 MPa respectively. Lignin modified (lignin = 22.4%) and delignified ash wood (lignin = 5.3%) had a wet strength of 13.9 MPa and 0.8 MPa respectively. Lignin modified pine had a wet strength of 14.4 MPa. Although ash, birch, and pine showed a significant difference between the wet strength of delignified and lignin modified wood samples, the wet strength difference for balsa wood was marginal. Delignified pine wood was too weak for strength testing. Höglund et al. (2020) compared bleaching to delignification in the production of ETW. While the transmittance showed little difference (90% and 85%), the haze of bleached ETW wood and delignified ETW wood varied greatly (36% and 63%). Zhu et al. (2016a) illustrated that the optical transmittance of delignified wood samples increased with increase in degree of delignification. For example, 33%, 50% and 100% delignified wood had transmittances of approx. 2%, 5% and 15%, respectively. These results were in agreement with Khalili et al. (2017), where the light transmittance values of 33%, 35%, 47%, 51%, and 64% delignified ETW was approx. 25%, 35%, 43%,47% and 50%, respectively. The tensile strength of 33%, 35%, 47%, 51% and 64% delignified ETW was 166 MPa, 171 MPa, 161 MPa, 159 MPa and 152 MPa, respectively. Foster et al. (2021) compared the water transport property in chemically modified ETW produced by peroxide-based lignin modification and chlorite-based lignin oxidation. The lignin modified and oxidised wood was further treated via acetylation, 2-hydroxyethyl methacrylate treated treatment and methacrylation. Lignin-modified ETW had lower diffusion coefficients (10.6 for untreated, 2.47 for acetylated, 1.88 methacrylated, 18.91 for

2-hydroxyethyl methacrylate treated) than lignin-oxidized ETWs (12.97 for untreated, 3.93 for acetylated, 5.47 for methacrylated, 46.9 for 2-hydroxyethyl methacrylate treated) at 4 °C due to its high lignin content that was water resistant (Foster et al. 2021). The diffusivity increased with increase in temperature for all ETWs produced because increased thermal energy facilitated faster transport of water into the ETW composite (Foster et al. 2021).

Type of infiltration polymer and compatibility with wood components

The infiltration polymer plays a major role in determining the structural, optical and functional properties of the ETW (Wang et al. 2021). A good polymer is one that has a refractive index that matches that of the wood components, which are cellulose (RI = 1.525), hemicellulose (RI = 1.532), and lignin (RI = 1.610) (Vasileva et al. 2018). Besides, the refractive index, the viscosity, compatibility and shrinkage of the polymer are important selection criteria (Li et al. 2018a). The polymer's ability to reduce the optical scattering of the wood may also lead to a desirable combination of high transmittance and low haze. In most studies, PMMA, epoxy resin, polyvinylpyrrolidone, *n*-butyl methacrylate, polystyrene, dibutylphthalate, iso-bornyl methacrylate, diallyl phthalate and poly vinylcarbazole and poly(acrylic acid) with refractive indices of approximately 1.49, 1.5, 1.53, 1.50, 1.59, 1.52, 1.48, 1.50, 1.68 and 1.45, respectively, are used (Fink 1992; Vasileva et al. 2018; Chen et al. 2020). Li et al. (2018c) reported that polymers had a higher transmittance of 95% compared to transparent wood despite the full infiltration of polymer into wood cell lumens. The decreased transmittance was due to interface bonding which resulted in interface gaps and created optical heterogeneity. The low refractive index of air (1.000) in the interface gaps resulted in light scattering hence decreased transmittance. The air gaps were caused by low compatibility between hydrophilic wood cells and hydrophobic polymers and the shrinkage of the polymer during polymerisation (Li et al. 2018c; Vasileva et al. 2018; Chen et al. 2019). The mechanical properties (in ascending order) of ETW composed of different polymers were: PMMA-ETW; fracture strength = 59.8 MPa and modulus 2720 MPa, epoxy-ETW; fracture strength = 23.4 MPa, modulus = 1220 MPa PVA-ETW-PG; fracture strength = 13.3 MPa, modulus = 260 MPa (Zhu et al. 2016b; Yu et al. 2017; Rao et al. 2019; Wang et al. 2019b). Correspondingly, pure PMMA (tensile strength = 55.4 MPa, modulus = 2900 MPa) followed by epoxy (tensile strength = 50.2 MPa, Young modulus = 2400 MPa) have the highest strength properties, whereas PVA (tensile strength = 48.4 MPa, Young modulus = 707.9 MPa) has the lowest values (Ibrahim and Hassan 2011; Gong et al. 2016; Yusof et al. 2016; Jain et al. 2017; Seghir and Pierron 2018). It can be concluded that the strength of the polymer positively contributes to the strength of ETW produced. Yue et al. (2021) reported transmittance values (wavelength = 600 nm) of 76.6%, 73.4%, and 64.6% for ETW composed of polyvinyl alcohol (PVOH), PVP and PMMA, respectively. A study to determine the extent to which transmittance can be improved when delignified wood is acetylated before polymer infiltration was conducted (Li et al. 2018c). Acetylated ETW had a high transmittance of 92% at a thickness of 1.5 mm, while non-acetylated ETW had a lower transmittance of 83%. In this case, the wood texture of acetylated EWT was less pronounced. This indicated improved compatibility between the wood and the PMMA polymer. It was observed that with an increase in the thickness of ETW, the transmittance decreased. However, the transmittance of acetylated ETW remained higher than non-acetylated ETW of the same thickness (Li et al. 2018c). In addition, an increase in the difference in transmittance between the acetylated and non-acetylated ETW of the same thickness was noted. Zhu et al. (2016a) opted for a biodegradable polymer, PVP, over epoxy resins which are made of toxic monomers such as bisphenol-A and epichlorohydrin. However, the resulting ETW lacked flexibility. In order to improve the flexibility of the PVP infiltrated ETW, a plasticing agent such as propylene glycol (PG) was used (Rao et al. 2019). Besides biodegradability, PVP is desirable due to its low cost, water solubility, low viscosity in water, excellent film forming property, toughness and transparency, with a refractive index of 1.48 (Wu et al. 2012; Mi et al. 2020b). The hydrophilic nature of PVP alleviated the need to use dehydrating chemicals such as ethanol and acetone in order to increase its compatibility with delignified wood. The thermal conductivities of ETW composed of different polymers had different conductivities, which were far less than the thermal conductivities of glass. For instance,

the thermal conductivities of PVA-ETW, PMMA-ETW, and Epoxy-ETW were reported to be 0.19 W m^{-1} K^{-1}, 0.23 W m^{-1} K^{-1} and 0.24 W m^{-1} K^{-1}, respectively (Li et al. 2017a, 2019b; Mi et al. 2020a, 2020b). Wachter et al. (2021) compared the extent of photo degradation of ETWs fabricated using two different polymers (methyl methacrylate, 2-hydroxyethyl methacrylate) over a period of 35 days exposed to monochromatic UV-C (λ—250 nm) radiation. The optical transmittance of methyl methacrylate-ETW reduced from 58 to 43%, whereas 2-hydroxyethyl methacrylate-ETW reduced from 69 to 57% within 7 days of exposure to UV radiation. Further increase in time resulted in a negligible decrease in optical transmittance (Wachter et al. 2021). It was concluded that decrease in optical properties of both types of ETW was caused by the degradation of both the acrylic polymers and the wood templates. The disadvantages of PVA-ETW were that it had a high solubility in water resulting in weight gain of ETW samples exposed to high humidity conditions. On the other hand, the solubility of PVA favours easy recycling of ETW and recovery of PVA (Rao et al. 2019). Höglund et al. (2020) infiltrated the bleached wood pores with a thiol-ene thermoset to prepare ETW with an optical transmittance of 90% and a haze of 36%. The thiol-ene thermoset network was prepared from thiol PETMP and trifunctional ene TATATO monomers by polymerisation. It was concluded that the adhesion of the thiol-ene polymer significantly contributed to the low haze and high transmittance instead of the wood-polymer matching refractive indices (Höglund et al. 2020).

Modification/functionalisation of ETW

The disadvantages of ETW, such as low transmittance caused by light scattering at the cellulose-polymer interface, and the loss of optical and mechanical integrity due to exposure to adverse weather conditions (e.g., rain, temperature etc.), can be overcome through functionalisation. The potential for modification and multi functionalities of wood and ETW is due to micro-scale channels and nanopores in the cell wall. Furthermore, functionalisation extends the applications of ETW. Various additives provide the wood composites functionalities, such as luminescence, conductivity, UV stability, aesthetics, fluorescence, stimuli responsiveness, electromagnetic shielding and magnetocaloric (Li et al. 2017b; Zhang et al. 2020). Bisht et al. (2021) fabricated UV resistant ETW by combing a UV absorber (2-(2H-Benzotriazol-2-yl)-4, 6- di-tert-pentylphenol) with an epoxy resin before infiltration into bleached wood. This led to photostable ETW that did not photodegrade nor change colour when exposed to UV light. Also, the UV absorber had no effect on the optical properties of the ETW. A comparative study showed that ETW without a UV absorber had a change in yellowness value of approximately 10, 20, and 25 after 25 h, 100 h and 250 h of UV exposure, respectively. In comparison, ETW containing 1.75% UV absorber content had a change in yellowness value of approximately 2, 5 and 10 after 25 h, 100 h and 250 h of UV exposure, respectively. Increasing UV exposure time resulted in increased photodegradation which was indicated by a decrease in light transmittance. For example, at a wavelength of 550 nm and 250 h UV exposure time, the percentage transmittance loss was 27.5%, 1.43%, and 0.96% for ETW with UV absorber concentrations of 0%, 1% and 1.75%, respectively (Bisht et al. 2021). Wang et al. (2019a) reported the fabrication of photochromic ETW with photo-switching of transmittance in the visible light region and colour tuning properties. The delignified wood was filled with a mixture of photochromic material 30,30-dimethyl-6-nitro-spiro[2H-1-benzopyran-2,20-indoline]-10-ethanol (DNSE) and pre-polymerized methyl methacrylate (MMA). The components of DNSE, spiropyran and merocyanine responded to UV light or green light. A similar study involved the fabrication of photochromic and fluorescent ETW with color switching properties from lignin modified basswood, methyl methacrylate (MMA) and a photoluminescent lanthanide-doped aluminum strontium oxide (Al-Qahtani et al. 2021). Chen et al. (2020) produced a flame-retardant transparent wood composite from pristine natural wood by delignification followed by polyimide infiltration and chemical imidisation. The transparent wood composite showed high mechanical strength (stress and modulus of 169 MPa and 2.11 GPa, respectively) in addition to outstanding flame retardancy characterised by the physical integrity of the composite during combustion. Compared to natural wood and polyimide film, where a shrinkage, twisting and formation of soft and loose

residue occurred, the ETW composite formed a visible layer of char on the residue, therefore, heat transfer between the flame and composite was prevented within 2 s. Cho et al. (2021) fabricated heat-shielding transparent wood by application of indium tin oxide on its surface. Balsa wood ($50 \times 50 \times 1.4$ mm^3) was delignified and infiltrated with epoxy to produce ETW with 80% light transmittance, dielectric constant of 3.344 and the loss tangent was observed at 0.0552. The addition of indium tin oxide resulted in heat shielding ETW with approximately 62% light transmittance. On the other hand, fabrication of heat shielding ETW by the addition of TiO_2 nanoparticles resulted in a higher transmittance and haze of 90% and 90%, respectively. The thermal conductivity was 0.3228 W m^- K^{-1} (Wu et al. 2022). Fu et al. (2018) fabricated luminescent ETW by delignification of wood veneers followed by compression, impregnation of PMMA combined with quantum dots lamination and polymerisation. In another study, Wang et al. (2021) fabricated 1 mm, 2 mm, and 3 mm thick programmable shape-memory transparent wood (PSMTW) from balsa wood (density 126 kg m^{-3}), using $NaClO_2$ under acidic conditions, followed by infiltration of epoxy vitrimers. Light transmittances of 75.7%, 61.8%, and 52.8% were reported for 1 mm, 2 mm, and 3 mm thick PSMTW, respectively, whereas the haze for all the ETW samples was approx. 95%. Gan et al. (2017a) endowed transparent wood with magnetic properties by adding RI-matching MMA and magnetic Fe_3O_4 nanoparticles into the delignified wood template for application in light-transmitting magnetic buildings and magneto-optical devices. The magnetisation of ETW increased with an increase in the concentration of Fe_3O_4 nanoparticles. However, the mechanical properties decreased with an increase in the concentration of the agglomeration and concentration of the nanoparticles in the cracks in the aggregates. Rao et al. (2019) produced flexible ETW with potential application as a light shaping diffuser by infiltration of aqueous propylene glycol (PG) and plasticised PVP into bleached wood veneers. A light transmittance as high as 80% and a haze of 90% were achieved at a ratio of 1:1 of PG and PVA. Images (Fig. 5) were used to demonstrate the flexibility of ETW (a) bent across the fibre direction; (b) bent across the perpendicular direction of fibre orientation; (c) twisted, and (d) rolled. Wang et al. (2022) also fabricated flexible ETW by polymerisation of EDCP in a delignified wood template via an epoxy-thiole reaction. The resulting ETW possessed plasticity, shape manipulation capability, good thermal insulation and optical properties. Bending tests were performed on the ETW of 2 mm thickness to measure the bending deformation angles. Stress was applied by an external force on the ETW to form curved shapes at 60 °C and fixation temperature of 0 °C to obtain a temporary shape and recovery observed within 30 min when the temperature was increased back to 60 °C. T-ETW was initially deformed to a temporary curved shape with an angle of 0°. Measurements showed gradual recovery to original rectangular shapes of the deformed T- ETW marked by an increase in bending deformation angles from 0° to 3°, 8°, 18°, 40°, 100°, 144° and 156° from after 0 s, 10 s, 30 s, 1 min, 2 min, 5 min, 10 min and 30 min recovery time, respectively (Wang et al. 2022). In the case of L-ETW, an increase in bending deformation angles from 0° to 3°, 14°, 39°, 91°, 161°, 166° and 170° from after 0 s, 10 s, 30 s, 1 min, 2 min, 5 min, 10 min and 30 min recovery time, respectively (Wang et al. 2022). Li et al. (2017b) produced luminescent transparent wood by the infiltration of quantum dots dispersed in a PMMA/oligomer liquid mixture. Yu et al. (2017) produced 5 mm thick heat shielding ETW from beech wood via NaOH,

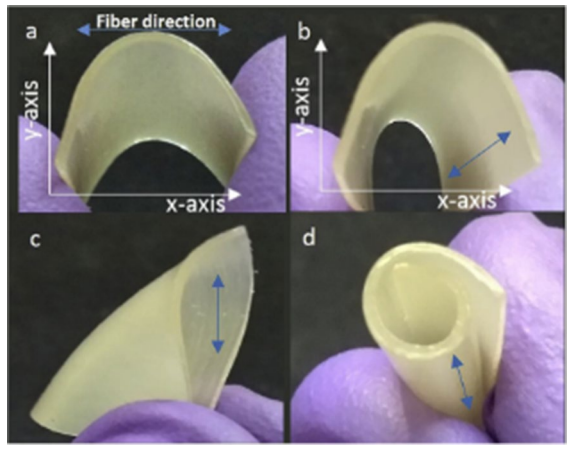

Fig. 5 Images showing the flexibility of ETW produced by infiltration of PG and PVA (a) (a) bent across the fibre direction; (b) bent across the perpendicular direction of fibre orientation; (c) twisted and (d) rolled. Reproduced with permission Copyright 2019, Elsevier (Rao et al. 2019)

Na_2SO_3 and H_2O_2 delignification process followed by infiltration of Cs_xWO_3/MMA mixture. Although the optical transmittance of ETW decreased with increased concentration of Cs_xWO_3, whereas the heat shielding ability increased, an optimum dosage of 0.03 wt% in the Cs_xWO_3/MMA mixed solution resulted in 72% transmittance and strength of 59.8 MPa and modulus of 2.72 GPa. Comparison of mechanical properties showed that transparent wood was much stronger (strength = 60.2 MPa, modulus = 2.67 GPa) than $CsxWO_3$/ETW (strength = 59.8 MPa and modulus 2.72 GPa), PMMA (strength = 39.6 MPa, modulus = 1.83 GPa) and natural wood (strength = 55.1 MPa, modulus = 5.67 GPa). The simulation test showed that Cs_xWO_3/ETW can be used as energy efficient smart windows (Yu et al. 2017). Hu et al. (2022) produced ETW with a very low thermal conductivity of 0.157 W m^{-1} K^{-1} after coating with a ZnO film via sonochemical deposition process. The low thermal conductive made the ZnO coated ETW ideal for glazing applications.

Applications

ETW can be tailor made to fit the specifications of applications. For instance, the thickness of ETW depends on the thickness of initial wood chosen. The mechanical and optical properties of ETW can be controlled by the optical (i.e. refractive index) and mechanical properties of the polymer infiltrated during fabrication. However, for large scale applications, the loss of optical transmittance of ETW of high thickness is a problem. Also, there is need to reduce polymer shrinkage during polymerization in the production of thick ETW (Li et al. 2018a). The applications of ETW are discussed in the following sections and a summary provided in Table 2.

Building materials

Incorporation of ETW instead of glass as a building material resulted in improved optical transmittance (85%), no glare effect, optical haze (> 95%), peculiar light guiding effect with large forward to back scattering ratio (scattering ratio of 9 for 0.5 cm thick ETW), good thermal insulation (i.e. thermal conductivity ~ 0.32 W m^{-1} K^{-1} and ~ 0.15 W m^{-1} K^{-1} in the cross plane), alleviated safety issues associated with glass, simple and fast fabrication and scalability (Li et al. 2016a). ETW preserves the original cellulose nanofibers of wood which contribute to anisotropic properties. Li et al. (2016a) demonstrated that when ETW is used as a roof top it maintains uniform lighting and a constant temperature inside the building. It was concluded that the application of ETW in a building created comfortable living conditions and reduces energy costs. Li et al. (2019c) used a real house simulation test to confirm the infrared-heat shielding ability and energy storage performance of ETW composed of $VO_2(M)@SiO_2$ and thermochromic microcapsules particles. The ETW was proposed to be suitable for building, furniture, thermal insulation, energy conversion, energy storage, and conservation.

Aesthetics material

Functionalisation of ETW extends its applications to decorative materials. For instance, addition of

Table 2 A summary of Applications of ETW

Application	References
Magnetic ETW	Gan et al. (2017a), Gan et al. (2017b)
Building components (rooftop and windows)	Yaddanapudi et al. (2017), Li et al. (2019c)
Smart windows	Samanta et al. (2021)
Flame retardant ETW	Chen et al. (2020)
Aesthetic material	Wang et al. (2019a), Mi et al. (2020a), Mi et al. (2020b), Hoglund et al. (2021)
Smartphone screen	Magrini et al. (2021)
Photovolaic	Zhu et al. (2016a)
Photovoltaic cells	Li et al. (2019b)

quantum dots to ETW resulted in multi colour luminescence that can be used for planar light sources, building construction elements and furniture (Li et al. 2017b). Yu et al. (2017) produced CsxWO$_3$-ETW with an optical transmittance of 86% and haze of 90%, temperature and humidity resistance (i.e. excellent shielding ability of near-infrared ranging from 780 to 2500 nm). Additionally, the mechanically properties (tensile strength = 60.1 MPa, and modulus = 2.72 GPa fracture strength = 59.8 MPa) of the CsxWO$_3$-ETW were favourable for heat shielding window applications. The transmittance of the CsxWO3/ETW was observed to increase slowly in high temperature (85 °C) and humidity conditions (90% RH). Model houses were developed to compare the thermoregulation effects of CsxWO$_3$/ETW to glass. After continuous application of solar radiation, the ordinary glass house model temperature increased from 21.5 °C to 41.5 °C whereas the CsxWO$_3$-ETW model increased from 21.6 °C to 26.8 °C (Yu et al. 2017). Mi et al. (2020a) produced aesthetic ETW with preserved wood patterns by spatial selectively removing lignin from Douglas fir (softwood). The aesthetic wood possessed good mechanical properties (strength = 91.95 MPa, toughness = 2.73 MJm^{-3}), low thermal conductivity (0.24Wm^{-1} K^{-1}), and excellent optical properties (transparency ~ 80%, optical haze ~ 93%). These properties are desirable for patterned ceilings, rooftops, transparent decorations, and indoor panels (Mi et al. 2020a). Wang et al. (2019a) fabricated photochromic ETW containing 3',3'-dimethyl-6-nitro-spiro[2H-1-benzopyran-2,2'-indoline]-1'-ethanol. The ETW exhibited a multi colour change under the illumination of light making it suitable for photo-switchable, and colourful smart windows (Wang et al. 2019a; Al-Qahtani et al. 2021).

Photovoltaic and optoelectronic devices

ETW are not only energy efficient but result in green disposable optoelectronic and photovoltaic devices (Zhu et al. 2016a). Fang et al. (2014) reported that a combination of high optical transparency and high optical haze is beneficial for solar cell substrates to adsorb active materials and increase the light scattering thereby ensuring solar cell efficiency. Zhu et al. (2016a) compared the efficiency of GaAs (Gallium arsenide) solar with or without attachment of ETW (optical transmittance of 90% and haze of 80%). The overall conversion efficiency of GaAs with and without ETW was 18.02% and 12.21% respectively. It was concluded that ETW was efficient in broadband light management which led to efficient light scattering and adsorption within the solar cell, hence the improved conversion efficiency. Li et al. (2019b) fabricated photovoltaic cells on transparent wood substrates which led to a power conversion efficiency of 16.8%.

Other applications

Addition of γ-Fe2O3@YVO4:Eu3 + and Fe3O4 nanoparticles has been reported to reported to endow ETW with magnetic properties that were desirable in applications such as electromagnetic interference shielding, LED lighting equipment, luminescent magnetic switches, and anti-counterfeiting facilities (Gan et al. 2017a, 2017b). ETW can be used in speciality applications such as smart phone screens (Magrini et al. 2021). Wang et al. (2022) produced ETW which possessed flexibility, solid shape plasticity, shape manipulation capabilities and unique guiding effects. The ETW was produced through polymerisation of epoxy-based dynamic covalent polymers into a delignified wood template. Applications such as curved or irregularly shaped glass, windows, ceilings, rooftops were suggested for the ETW (Wang et al. 2022). Bi et al. (2018) fabricated multi colour emission ETW containing carbon dots. The properties of the multi colour emission ETW exhibited excellent optical and mechanical properties desirable for use as encapsulating material for white light-emitting diodes.

Conclusion

Generally, ETW was manufactured in two steps, i.e., delignification of wood and infiltration of RI matching polymers. The main focus in ETW production was reducing lignin or lignin chromophores while maintaining the structural integrity of wood, eliminating polymer cell wall interface gaps by improving polymer infiltration, improving the short and long term integrity of ETW, especially in outdoor applications, by surface modification, and exploiting the natural characteristics of wood to the benefit of the ETW (e.g. aesthetic patterns) (Jia et al. 2019; Mi et al. 2020a).

The studies in this review revealed that wood of high density is desirable in the production of ETW because of its strength, even after delignification. Also, the ETW produced had high tensile strength. However, the disadvantages of high-density wood were long delignification time and low optical transmittance of ETW produced.

A higher volume fraction of cellulose in wood resulted in high mechanical strength and low optical transmittance. The cellulose volume fraction was a tunable property which could be increased by the compression of delignified wood template.

Longitudinal ETW had higher mechanical strength than radial ETW. On the contrary, radial delignified wood had greater mechanical properties than delignified longitudinal wood. Radial ETW had higher optical transmittance than longitudinal ETW. The conclusion.

Radial ETW and axial ETW had thermal conductivities of 0.24 W m^{-1} K^{-1} and 0.41 W m^{-1} K^{-1}. It was concluded that restrained heat transfer in the radial direction results in greater light scattering than in the axial direction.

In the case of delignification, the optical transmittance of delignified wood samples increased with increase in the degree of delignification however mechanical properties of the ETW were negatively affected by increased levels of delignification. The tensile strength decreased with a decrease in lignin content in ETW samples.

ETW produced by infiltration of PMMA had the highest mechanical properties. It can be concluded that the strength of the polymer positively contributes to the strength of ETW produced. However, the low optical properties had to be improved by acetylation. The applications of ETW include solar cells, windows, decorative materials, and screens. The main disadvantages of ETW are the limited scalability. Only ETW with a thickness less than 1 cm thick was successfully produced with acceptable optical properties (transmittance = 60%) (Li et al. 2018c). Although the short-term durability of ETW was proven, long term durability, especially in outdoor applications, requires further research.

Acknowledgments The authors acknowledge the Council for Scientific and Industrial Research, Biorefinery Industry Development Facility, South Africa for supporting this work.

Author contributions All authors contributed to the review article. The literature study and the first draft of the article were written by Thabisile Jele, and all authors reviewed, revised, and made relevant contributions and suggestions for the submitted manuscript. All authors read and approved the final manuscript.

Funding Open access funding provided by University of KwaZulu-Natal. Authors wish to acknowledge funding received from the South African Technology Innovation Agency (TIA) under the South African Forestry Bio-economy Innovation Cluster (FBIC), Programme 2 and the CSIR Parliamentary Grant funding 2022/2023.

Declarations

Competing interests The authors declare no competing interests.

Consent for publication All authors consent to the publication of this review.

References

Al-Qahtani S, Aljuhani E, Felaly R, Alkhamis K, Alkabli J, Munshi A, El-Metwaly N (2021) Development of photoluminescent translucent wood toward photochromic smart window applications. Indl Eng Chemy Res 60:8340–8350. https://doi.org/10.1021/acs.iecr.1c01603

Bi Z, Li T, Su H, Ni Y, Yan L (2018) Transparent wood film incorporating carbon dots as encapsulating material for white light-emitting diodes. ACS Sustain Chem Eng 6:9314–9323. https://doi.org/10.1021/acssuschemeng.8b01618.s001

Bisht P, Pandey KK, Barshilia HC (2021) Photostable transparent wood composite functionalized with an UV-absorber. Polym Degrad Stab 189:109600. https://doi.org/10.1016/j.polymdegradstab.2021.109600

Chen H, Baitenov A, Li Y, Vasileva E, Popov S, Sychugov I, Yan M, Berglund L (2019) Thickness dependence of optical transmittance of transparent wood: chemical modification effects. ACS Appl Mater Interfaces 11:35451–35457. https://doi.org/10.1021/acsami.9b11816

Chen L, Xu Z, Wang F, Duan G, Xu W, Zhang G, Yang H, Liu J, Jiang S (2020) A flame-retardant and transparent wood/polyimide composite with excellent mechanical strength. Compos Commun 20:100355. https://doi.org/10.1016/j.coco.2020.05.001

Cho SS, Song SH, Hong IP (2021) Analysis of the electromagnetic properties of eco-friendly transparent wood. Microw Opt Technol Lett 63:2237–2241. https://doi.org/10.1002/mop.32385

Chutturi M, Gillela S, Yadav SM, Wibowo ES, Sihag K, Rangppa SM, Bhuyar P, Siengchin S, Antov P, Kristak LJ (2022) A comprehensive review of the synthesis strategies, properties, and applications of transparent wood as a renewable and sustainable resource. Sci Total Environ 864:161067

Cl M, Li Y, Chen H, Yan M, Berglund LA (2019) Transparent wood for thermal energy storage and reversible optical transmittance. ACS Appl Mater Interfaces 11:20465–20472. https://doi.org/10.1021/acsami.9b05525.s001

EIA (2016) U.S. Energy Information Administration International Energy Outlook

Fang Z, Zhu H, Yuan Y, Ha D, Zhu S, Preston C, Chen Q, Li Y, Han X, Lee S, Chen G (2014) Novel nanostructured paper with ultrahigh transparency and ultrahigh haze for solar cells. Nano Lett 14(2):765–773

Fink S (1992) Transparent wood—a new approach in the functional study of wood structure. Holzforschung. https://doi.org/10.1515/hfsg.1992.46.5.403

Foster KE, Hess KM, Miyake GM, Srubar WV III (2019) Optical properties and mechanical modeling of acetylated transparent wood composite laminates. J Mater 12:2256. https://doi.org/10.3390/ma12142256

Foster KE, Jones R, Miyake GM, Srubar WV III (2021) Mechanics, optics, and thermodynamics of water transport in chemically modified transparent wood composites. Compos Sci Technol 208:108737. https://doi.org/10.1016/j.compscitech.2021.108737

Fu Q, Yan M, Jungstedt E, Yang X, Li Y, Berglund LA (2018) Transparent plywood as a load-bearing and luminescent biocomposite. Compos Sci Technol 164:296–303. https://doi.org/10.1016/j.compscitech.2018.06.001

Gan W, Gao L, Xiao S, Zhang W, Zhan X, Li J (2017a) Transparent magnetic wood composites based on immobilizing Fe_3O_4 nanoparticles into a delignified wood template. J Mater Sci 52:3321–3329. https://doi.org/10.1007/s10853-016-0619-8

Gan W, Xiao S, Gao L, Gao R, Li J, Zhan X (2017b) Luminescent and transparent wood composites fabricated by poly (methyl methacrylate) and γ-Fe_2O_3@ YVO_4: Eu^{3+} nanoparticle impregnation. ACS Sustain Chem Eng 5:3855–3862. https://doi.org/10.1021/acssuschemeng.6b02985.s001

Gong L-X, Pei Y-B, Han Q-Y, Zhao L, Wu L-B, Jiang J-X, Tang L-C (2016) Polymer grafted reduced graphene oxide sheets for improving stress transfer in polymer composites. Compos Sci Technol 134:144–152. https://doi.org/10.1016/j.compscitech.2016.08.014

Höglund M, Johansson M, Sychugov I, Berglund LA (2020) Transparent wood biocomposites by fast UV-curing for reduced light-scattering through wood/thiol–ene interface design. ACS Appl Mater Interfaces 12:46914–46922. https://doi.org/10.1021/acsami.0c12505.s001

Hoglund M, Garemark J, Nero M, Willhammar T, Popov S, Berglund LA (2021) Facile processing of transparent wood nanocomposites with structural color from plasmonic nanoparticles. Chem Mater 33(10):3736–3745

Hu X, Zhang Y, Zhang J, Yang H, Wang F, Bin F, Noor N (2022) Sonochemically-coated transparent wood with ZnO: Passive radiative cooling materials for energy saving applications. Renew Energy 193:398–406. https://doi.org/10.1016/j.renene.2022.05.008

Ibrahim AA, Hassan MF (2011) Study the mechanical properties of epoxy resin reinforced with silica (quartz) and alumina particles. Iraqi J Mech Mater Eng 11

Jain N, Singh VK, Chauhan S (2017) A review on mechanical and water absorption properties of polyvinyl alcohol based composites/films. J Mech Behav Biomed Mater 26:213–222. https://doi.org/10.1515/jmbm-2017-0027

Jia C, Chen C, Mi R, Li T, Dai J, Yang Z, Pei Y, He S, Bian H, Jang S-H (2019) Clear wood toward high-performance building materials. ACS Nano 13:9993–10001. https://doi.org/10.1021/acsnano.9b00089.s001

Jungstedt E, Montanari C, Östlund S, Berglund L (2020) Mechanical properties of transparent high strength biocomposites from delignified wood veneer. Compos Part A Appl Sci 133:105853. https://doi.org/10.1016/j.compositesa.2020.105853

Kanócz J, Bajzecerová V, Karl'a V (2020) Analysis of mechanical properties of I-beam with web from transparent wood. IOP Conference Series: Materials Science and Engineering. IOP Publishing, 012017

Khalili P, Tshai K, Hui D, Kong I (2017) Synergistic of ammonium polyphosphate and alumina trihydrate as fire retardants for natural fiber reinforced epoxy composite. Compos B Eng 114:101–110. https://doi.org/10.1016/j.compositesb.2017.01.049

Lang AW, Li Y, De Keersmaecker M, Shen DE, Österholm AM, Berglund L, Reynolds JR (2018) Transparent wood smart windows: polymer electrochromic devices based on poly (3,4-ethylenedioxythiophene): poly (styrene sulfonate) electrodes. Chemsuschem 11:854–863. https://doi.org/10.1002/cssc.201702026

Li T, Zhu M, Yang Z, Song J, Dai J, Yao Y, Luo W, Pastel G, Yang B, Hu L (2016a) Wood composite as an energy efficient building material: Guided sunlight transmittance and effective thermal insulation. Adv Energy Mater 6:1601122. https://doi.org/10.1002/aenm.201601122

Li Y, Fu Q, Yu S, Yan M, Berglund L (2016b) Optically transparent wood from a nanoporous cellulosic template: combining functional and structural performance. Biomacromol 17:1358–1364. https://doi.org/10.1021/acs.biomac.6b00145.s001

Li Y, Fu Q, Rojas R, Yan M, Lawoko M, Berglund L (2017a) Lignin-retaining transparent wood. Chemsuschem 10:3445–3451. https://doi.org/10.1002/cssc.201701089

Li Y, Yu S, Veinot JG, Linnros J, Berglund L, Sychugov I (2017b) Luminescent transparent wood. Adv Opt Mater 5:1600834. https://doi.org/10.1002/adom.201600834

Li Y, Fu Q, Yang X, Berglund L (2018a) Transparent wood for functional and structural applications. Philos Trans R Soc 376:20170182. https://doi.org/10.1098/rsta.2017.0182

Li Y, Vasileva E, Sychugov I, Popov S, Berglund L (2018b) Optically transparent wood: recent progress, opportunities, and challenges. Adv Opt Mater 6:1800059. https://doi.org/10.1002/adom.201800059

Li Y, Yang X, Fu Q, Rojas R, Yan M, Berglund L (2018c) Towards centimeter thick transparent wood through interface manipulation. J Mater Chem 6:1094–1101. https://doi.org/10.1039/c7ta09973h

Li H, Guo X, He Y, Zheng R (2019a) A green steam-modified delignification method to prepare low-lignin delignified wood for thick, large highly transparent wood composites. Mater Res 34:932–940. https://doi.org/10.1557/jmr.2018.466

Li Y, Cheng M, Jungstedt E, Xu B, Sun L, Berglund L (2019b) Optically transparent wood substrate for perovskite solar cells. ACS Sustain Chem Eng 7:6061–6067. https://doi.org/10.1021/acssuschemeng.8b06248.s001

Li Y, Gao R, Li J (2019c) Energy saving wood composite with temperature regulatory ability and thermoresponsive performance. Eur Polym J 118:163–169. https://doi.org/10.1016/j.eurpolymj.2019.05.050

Magrini T, Bouville F, Studart AR (2021) Transparent materials with stiff and tough hierarchical structures. Open Ceram 6:100109. https://doi.org/10.1016/j.oceram.2021.100109

Mi R, Chen C, Keplinger T, Pei Y, He S, Liu D, Li J, Dai J, Hitz E, Yang B (2020a) Scalable aesthetic transparent wood for energy efficient buildings. Nat Commun 11:1–9. https://doi.org/10.1038/s41467-020-17513-w

Mi R, Li T, Dalgo D, Chen C, Kuang Y, He S, Zhao X, Xie W, Gan W, Zhu J (2020b) A clear, strong, and thermally insulated transparent wood for energy efficient windows. Adv Funct Mater 30:1907511. https://doi.org/10.1002/adfm.202001291

Montanari C, Ogawa Y, Olsén P, Berglund LA (2021) High performance, fully bio-based, and optically transparent wood biocomposites. Adv Sci 8:2100559. https://doi.org/10.1002/advs.202100559

Qin J, Li X, Shao Y, Shi K, Zhao X, Feng T, Hu Y (2018) Optimization of delignification process for efficient preparation of transparent wood with high strength and high transmittance. Vacuum 158:158–165. https://doi.org/10.1016/j.vacuum.2018.09.058

Qiu Z, Xiao Z, Gao L, Li J, Wang H, Wang Y, Xie Y (2019) Transparent wood bearing a shielding effect to infrared heat and ultraviolet via incorporation of modified antimony-doped tin oxide nanoparticles. Compos Sci Technol 172:43–48. https://doi.org/10.1016/j.compscitech.2019.01.005

Rao ANS, Nagarajappa GB, Nair S, Chathoth AM, Pandey KK (2019) Flexible transparent wood prepared from poplar veneer and polyvinyl alcohol. Compos Sci Technol 182:107719. https://doi.org/10.1016/j.compscitech.2019.107719

Samanta A, Chen H, Samanta P, Popov S, Sychugov I, Berglund L (2021) Reversible dual-stimuli-responsive chromic transparent wood biocomposites for smart window applications. ACS Appl Mater Interfaces 13:3270–3277

Seghir R, Pierron F (2018) A novel image-based ultrasonic test to map material mechanical properties at high strain-rates. Exp Mech 58:183–206. https://doi.org/10.1007/s11340-017-0329-4

United Nations Environment Programme (2017) Global Status Report 2017 - Towards a Zero-Emission, Efficient, and Resilient Buildings and Construction Sector

Vasileva E, Chen H, Li Y, Sychugov I, Yan M, Berglund L, Popov S (2018) Light scattering by structurally anisotropic media: a benchmark with transparent wood. Adv Opt Mater 6:1800999. https://doi.org/10.1002/adom.201800999

Wachter I, Štefko T, Rantuch P, Martinka J, Pastierová A (2021) Effect of UV radiation on optical properties and hardness of transparent wood. Polymers 13:2067. https://doi.org/10.3390/polym13132067

Wan C, Liu X, Huang Q, Cheng W, Su J, Wu Y (2021) A brief review of transparent wood: synthetic strategy, functionalization and applications. Curr Org Synth 18:615–623. https://doi.org/10.2174/1570179418666210614141032

Wang X, Zhan T, Liu Y, Shi J, Pan B, Zhang Y, Cai L, Shi SQ (2018) Large-size transparent wood for energy-saving building applications. Chemsuschem 11:4086–4093. https://doi.org/10.1002/cssc.201801826

Wang L, Liu Y, Zhan X, Luo D, Sun X (2019a) Photochromic transparent wood for photo-switchable smart window applications. J Mater Chem 7:8649–8654. https://doi.org/10.1039/c9tc02076d

Wang M, Li R, Chen G, Zhou S, Feng X, Chen Y, He M, Liu D, Song T, Qi H (2019b) Highly stretchable, transparent, and conductive wood fabricated by in situ photopolymerization with polymerizable deep eutectic solvents. ACS Appl Mater Interfaces 11:14313–14321. https://doi.org/10.1021/acsami.9b00728.s001

Wang K, Dong Y, Ling Z, Liu X, Shi SQ, Li J (2021) Transparent wood developed by introducing epoxy vitrimers into a delignified wood template. Compos Sci Technol 207:108690. https://doi.org/10.1016/j.compscitech.2021.108690

Wang K, Liu X, Dong Y, Ling Z, Cai Y, Tian D, Fang Z, Li J (2022) Editable shape-memory transparent wood based on epoxy-based dynamic covalent polymer with excellent optical and thermal management for smart building materials. Cellulose 29:7955–7972. https://doi.org/10.1007/s10570-022-04754-9

Wu W, Tian H, Xiang A (2012) Influence of polyol plasticizers on the properties of polyvinyl alcohol films fabricated by melt processing. J Polym Environ 20:63–69. https://doi.org/10.1007/s10924-011-0364-7

Wu J, Wu Y, Yang F, Tang C, Huang Q, Zhang J (2019a) Impact of delignification on morphological, optical and mechanical properties of transparent wood. Compos Part A Appl Sci 117:324–331. https://doi.org/10.1016/j.compositesa.2018.12.004

Wu J, Wu Y, Yang F, Tang C, Huang Q, Zhang J (2019b) Impact of delignification on morphological, optical and mechanical properties of transparent wood. Compos Part A Appl Sci Manuf 117:324–331

Wu Y, Wu J, Yang F, Tang C, Huang Q (2019c) Effect of H2O2 bleaching treatment on the properties of finished

transparent wood. Polymers 11:776. https://doi.org/10.3390/polym11050776

Wu Y, Zhou J, Huang Q, Yang F, Wang Y, Wang J (2020) Study on the properties of partially transparent wood under different delignification processes. Polymers 12:661. https://doi.org/10.3390/polym12030661

Wu Y, Zhou J, Yang F, Wang Y, Wang J, Zhang J (2021) A strong multilayered transparent wood with natural wood color and texture. J Mater Sci 56:8000–8013. https://doi.org/10.1007/s10853-021-05833-1

Wu T, Xu Y, Cui Z, Li H, Wang K, Kang L, Cai Y, Li J, Tian D (2022) Efficient heat shielding and ultraviolet isolating transparent wood via in situ generation of TiO_2 nanoparticles. ACS Sustain Chem Eng. https://doi.org/10.1021/acssuschemeng.2c04000.s001

Xia Q, Chen C, Li T, He S, Gao J, Wang X, Hu L (2021) Solar-assisted fabrication of large-scale, patternable transparent wood. Sci Adv 7:eabd7342. https://doi.org/10.1126/sciadv.abd7342

Yaddanapudi HS, Hickerson N, Saini S, Tiwari A (2017) Fabrication and characterization of transparent wood for next generation smart building applications. Vacuum 146:649–654. https://doi.org/10.1016/j.vacuum.2017.01.016

Yu Z, Yao Y, Yao J, Zhang L, Chen Z, Gao Y, Luo H (2017) Transparent wood containing Cs x WO_3 nanoparticles for heat-shielding window applications. J Mater Chem 5:6019–6024. https://doi.org/10.1039/c7ta00261k

Yue D, Fu G, Jin Z (2021) Transparent wood prepared by polymer impregnation of rubber wood (*Hevea brasiliensis* Muell.Arg). BioResources. https://doi.org/10.5376/biores.16.2.2491-2502

Yusof NSM, Dewi DEO, Salih NM, Supriyanto E, Syahrom A, Faudzi AAM (2016) Epoxy resin characterization for imaging phantom: X-ray, textural, and mechanical properties. In: IEEE EMBS conference on biomedical engineering sciences, pp 617–622. https://doi.org/10.1109/iecbes.2016.7843523

Zhang L, Wang A, Zhu T, Chen Z, Wu Y, Gao Y (2020) Transparent wood composites fabricated by impregnation of epoxy resin and W-doped VO2 nanoparticles for application in energy-saving windows. ACS Appl Mater Interfaces 12:34777–34783. https://doi.org/10.1021/acsami.0c06494.s001

Zhu M, Li T, Davis CS, Yao Y, Dai J, Wang Y, AlQatari F, Gilman JW, Hu L (2016a) Transparent and haze wood composites for highly efficient broadband light management in solar cells. Nano Energy 26:332–339. https://doi.org/10.1016/j.nanoen.2016.05.020

Zhu M, Song J, Li T, Gong A, Wang Y, Dai J, Yao Y, Luo W, Henderson D, Hu L (2016b) Highly anisotropic, highly transparent wood composites. J Adv Mater 28:5181–5187. https://doi.org/10.1002/adma.201600427

Zou F, Li H, Dong Y, Tewari GC, Vapaavuori J (2022) Optically transparent pectin/poly (methyl methacrylate) composite with thermal insulation and UV blocking properties based on anisotropic pectin cryogel. J Chem Eng 439:135738. https://doi.org/10.1016/j.cej.2022.135738